# Calcineurin/Nfat signaling is required for perinatal lung maturation and function

Vrushank Davé,[1] Tawanna Childs,[1] Yan Xu,[1] Machiko Ikegami,[1] Valérie Besnard,[1] Yutaka Maeda,[1] Susan E. Wert,[1] Joel R. Neilson,[2] Gerald R. Crabtree,[2] and Jeffrey A. Whitsett[1]

[1]Section of Neonatology, Perinatal and Pulmonary Biology, Cincinnati Children's Hospital Medical Center, University of Cincinnati College of Medicine, Cincinnati, Ohio, USA. [2]Departments of Pathology and Developmental Biology, Howard Hughes Medical Institute, Stanford University Medical School, Palo Alto, California, USA.

**Pulmonary surfactant proteins and lipids are required for lung function after birth. Lung immaturity and resultant surfactant deficiency cause respiratory distress syndrome, a common disorder contributing to morbidity and mortality in preterm infants. Surfactant CA synthesis increases prior to birth in association with formation of the alveoli that mediate efficient gas exchange. To identify mechanisms controlling perinatal lung maturation, the *Calcineurin b1* (*Cnb1*) gene was deleted in the respiratory epithelium of the fetal mouse. Deletion of *Cnb1* caused respiratory failure after birth and inhibited the structural maturation of the peripheral lung. Synthesis of surfactant and a lamellar body–associated protein, ABC transporter A3 (ABCA3), was decreased prior to birth. Nuclear factor of activated T cells (Nfat) calcineurin-dependent 3 (Nfatc3), a transcription factor modulated by calcineurin, was identified as a direct activator of *Sftpa*, *Sftpb*, *Sftpc*, *Abca3*, *Foxa1*, and *Foxa2* genes. The calcineurin/Nfat pathway controls the morphologic maturation of lungs prior to birth and regulates expression of genes involved in surfactant homeostasis that are critical for adaptation to air breathing.**

## Introduction

In late gestation, the fetal lung undergoes the structural and functional maturation required for adaptation to air breathing at birth. The respiratory saccules dilate, the mesenchyme thins, and the vascular bed grows into close apposition to squamous type I respiratory epithelial cells to form an efficient gas exchange surface required for respiration after birth (1). Cuboidal type II cells undergo marked ultrastructural and biochemical changes, including depletion of glycogen, increased surfactant protein and lipid synthesis, increased numbers of lamellar bodies, and secretion of surfactant into the air spaces. Surfactant reduces surface tension at the air-liquid interface and is required for pulmonary homeostasis at birth (2). Preterm birth or dysregulation of these processes result in pulmonary immaturity and surfactant deficiency, causing respiratory distress syndrome (RDS), a common disorder contributing to morbidity and mortality in preterm infants. Mechanisms controlling perinatal lung maturation and surfactant homeostasis are poorly understood and complex, mediated by autocrine-paracrine and endocrine signaling, including cell-cell and matrix-cell interactions (3).

A number of signaling and transcriptional programs are required in early lung morphogenesis and respiratory epithelial differentiation (4, 5). The important role of prenatal glucocorticoids that are used for prevention of RDS emphasizes the importance and utility of regulating gene transcription to improve lung maturation (6, 7). Knowledge of molecular pathways coordinating perinatal lung maturation and surfactant homeostasis is limited to the identification of mutations in *SFTPC*, *SFTPB*, and *ABC transporter A3* (*ABCA3*)

transporter genes that cause respiratory failure at birth in humans (5, 8). The identification of molecular pathways that enhance epithelial maturation in late gestation to facilitate perinatal lung function represents an important strategy for development of new therapies for prevention or treatment of RDS in preterm infants.

Calcineurin (Cn) is a $Ca^{2+}$/calmodulin-dependent serine-threonine protein phosphatase involved in many physiological processes (9). Cn exists as a heterodimer containing a 61-kDa catalytic A subunit (CnA) and a 19-kDa subunit (CnB) that binds calcium. In the cytosol, Cn is bound to calmodulin (CaM), forming a trimer. A rise in cytosolic $Ca^{2+}$ concentration following a signaling event leads to a conformational change in CaM and CnB that is essential for phosphatase activity of CnA. In vertebrates, 3 genes encode the catalytic subunit (*CnAα*, *CnAβ*, and *CnAγ*), while 2 genes encode the regulatory subunit (*CnB1* and *CnB2*) (10). The *CnAα*, *CnAβ*, and *CnB1* genes are expressed ubiquitously, while *CnAγ* and *CnB2* are expressed in the brain and testis (10). Cn directly dephosphorylates a family of Rel-like homology–containing transcription factors called nuclear factors of activated T cells (Nfats) within the cytoplasm and promotes the translocation of these factors into the nucleus, where they interact with other transcriptional partners and participate in the transcriptional regulation of diverse genes (9). In addition to established functions of Nfats in the immune and cardiovascular system, Nfats have recently been identified to play critical roles in vertebrate organogenesis and cellular processes in several tissues (9). The 4 Nfat genes (Nfatc1–Nfatc4) arose at the origin of vertebrates, implying that they have evolved for the development of vertebrate-specific functions such as complex nervous, immune, and cardiovascular systems (e.g., the 4-chambered heart) (11). The lung evolved relatively late in higher vertebrates; therefore, it is not surprising that the Nfat pathway might play important roles in lung formation and function. In a recent study, we found that Nfatc3 directly interacted with thyroid transcription factor 1 (TTF-1), a homeodomain-containing transcription factor critical for expression of surfactant proteins in the lung (12). Consistent
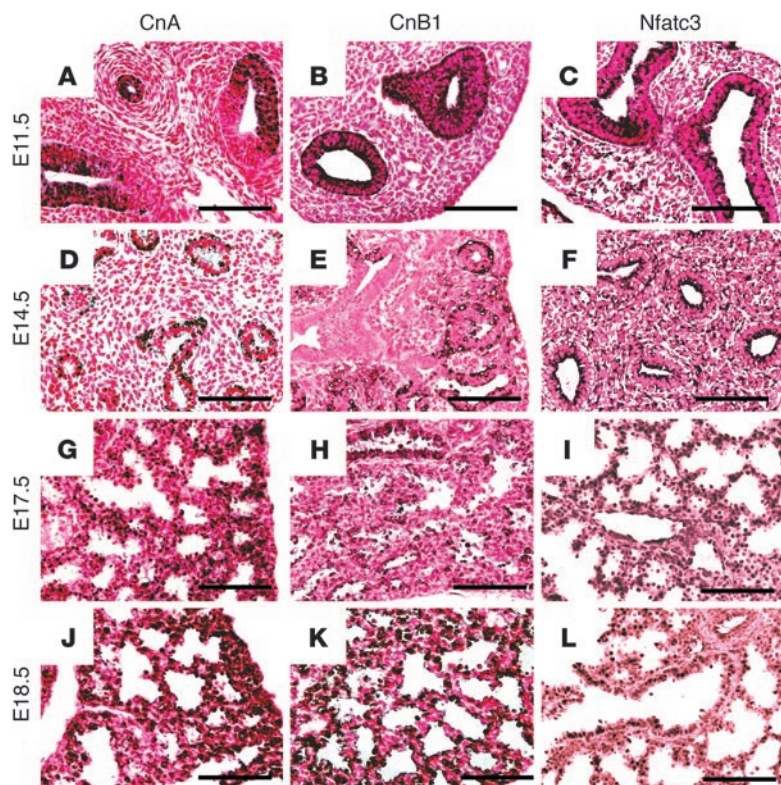
CnA          CnB1          Nfatc3

**Figure 1**
Components of the Cn/Nfat pathway during lung development. Immunostaining of CnA, CnB1, and its effector Nfatc3 in fetal mouse lungs from E11.5 to E18.5. (**A**) CnA was restricted to epithelial cells of the lung buds at E11.5. (**D**) At E14.5 CnA was detected in apical-basal membranes of the epithelial cells. (**G** and **J**) At E17.5–E18.5, CnA was expressed in both the epithelium and the mesenchyme. (**B** and **E**) CnB1 was detected in apical-basal regions of epithelial cells at E11.5 and E14.5, with intense staining in the peripheral lung tubules at E14.5. (**H** and **K**) At E17.5–E18.5, CnB1 was detected in both the mesenchyme and the epithelium. (**C** and **F**) Nfatc3 was detected in apical membranes of respiratory epithelial cells and mesenchyme at E11.5 and E14.5. (**I** and **L**) Nuclear Nfatc3 staining was observed in epithelial, endothelial, and mesenchymal cells at E17.5 and E18.5. Scale bars: 100 μm.

with a potential role for the Cn/Nfat signaling pathway in the lung, Nfatc3 and CnB1 were identified in the respiratory epithelium of the fetal mouse lung (12). To determine the potential role of Cn/Nfat signaling in perinatal lung maturation and function, here we selectively deleted the mouse *Cnb1* gene in the developing respiratory epithelium. Deletion of the *Cnb1* gene in the respiratory epithelium caused respiratory distress and death associated with morphological and biochemical immaturity of the lung.

## Results

*Expression of components of the Cn/Nfat pathway during lung development.* Expression of Cn/Nfat signaling components was assessed by immunostaining in the mouse lung from E11.5 to birth. Both CnA and CnB1 were detected in the apical and basal regions of respiratory epithelial cells at E11.5 and persisted until the day of birth at E18.5 (Figure 1). Nfatc3 was coexpressed with CnA and CnB1 in respiratory epithelial cells. In early lung buds (E11.5–E14.5), Nfatc3 was detected in the apical membrane of the respiratory epithelium and the mesenchyme. In late gestatation, Nfatc3 staining was predominantly nuclear, suggesting its activation by Cn and nuclear translocation. Expression of Nfatc4 was not detected in the lung. Nfatc1 was detected only in the pulmonary mesenchyme (data not shown), and Nfatc2 was not expressed in type II epithelial cells (12), supporting the concept that Nfatc3 is the potential transcriptional effector of Cn in the respiratory epithelium.

*Lung epithelial cell–specific deletion of Cnb1.* Triple-transgenic mice harboring *loxP*-flanked exons III–V of the regulatory subunit of the Cn gene *Cnb1* (*Cnb1flox/flox*), *SP-C–rtTAtg/–*, and *TetO-Cretg/tg* were produced in which *Cnb1* was selectively deleted in the respiratory epithelium following administration of doxycycline to the dam (Figure 2A). Since *Cnb1* is expressed early in embryonic lung

epithelium (E11.5), we used the human *SFTPC* gene promoter that is active in the early embryonic lung epithelial cells (13). In the presence of doxycycline, reverse tetracycline transactivator (rtTA) bound to the TetO promoter and activated expression of Cre recombinase, deleting exons III, IV, and V of the *Cnb1* gene (Figure 2A) and producing *Cnb1Δ/Δ* mice. At birth, genotype analysis (Figure 2B) demonstrated the transmission of the genes as predicted by Mendelian inheritance. In *Cnb1Δ/Δ* mice, while whole body weight was unaltered, the lung weight–to–body weight ratio was decreased by 10% (Figure 2D). Mice expressing *rtTA* or *Cre* genes without the *Cnb1flox/flox* allele from the time of conception to birth had a normal phenotype. No lung abnormalities were detected in mice expressing rtTA alone; therefore, these mice were used for further breeding.

*Cn/Nfat signaling components after Cnb1 deletion in the respiratory epithelium.* Absence of CnB1 staining was observed at E16.5 and E18.5 in lungs from *Cnb1Δ/Δ* mice (Figure 2, C and F). Loss of CnB1 correlated with sites of Cre expression (Figure 2F). CnB1 staining was not altered in control *Cnb1flox/flox* littermates (Figure 2F). During normal lung development, CnA and CnB1 were coordinately expressed in the respiratory epithelium (Figure 1). Deletion of *Cnb1* did not affect the sites or intensity of staining of CnA or Nfatc3 at E18.5 (Figure 2F), suggesting that Cn does not regulate CnA or Nfatc3 in the respiratory epithelium.

*Function of the Cn/Nfat pathway is required for lung maturation and perinatal survival.* Deletion of *Cnb1* caused respiratory failure within 6 hours to 2 days after birth. While branching morphogenesis of the lung was apparently normal in *Cnb1Δ/Δ* mice at E16.5, decreased sacculation was observed at E17.5 and persisted at E18.5 (Figure 2E). The pulmonary mesenchyme failed to thin, and peripheral saccules were not septated, findings consistent with pulmonary immaturity. Squamous type I cells were decreased or absent (Figure 3F), and cuboidal type II epithelial cells remained glycogen rich, also consistent with pulmonary immaturity (Figure 3G). Lungs of control littermates consisted of dilated peripheral lung saccules with thinning of mesenchyme and differentiation of squamous type I and cuboidal type II epithelium (Figure 2E and Figure 3F), typical of normal lung maturation in late gestation. Thus, deletion of the *Cnb1* gene impaired morphological maturation of the lung. Nfatc1 staining was detected in the developing pulmonary vasculature of
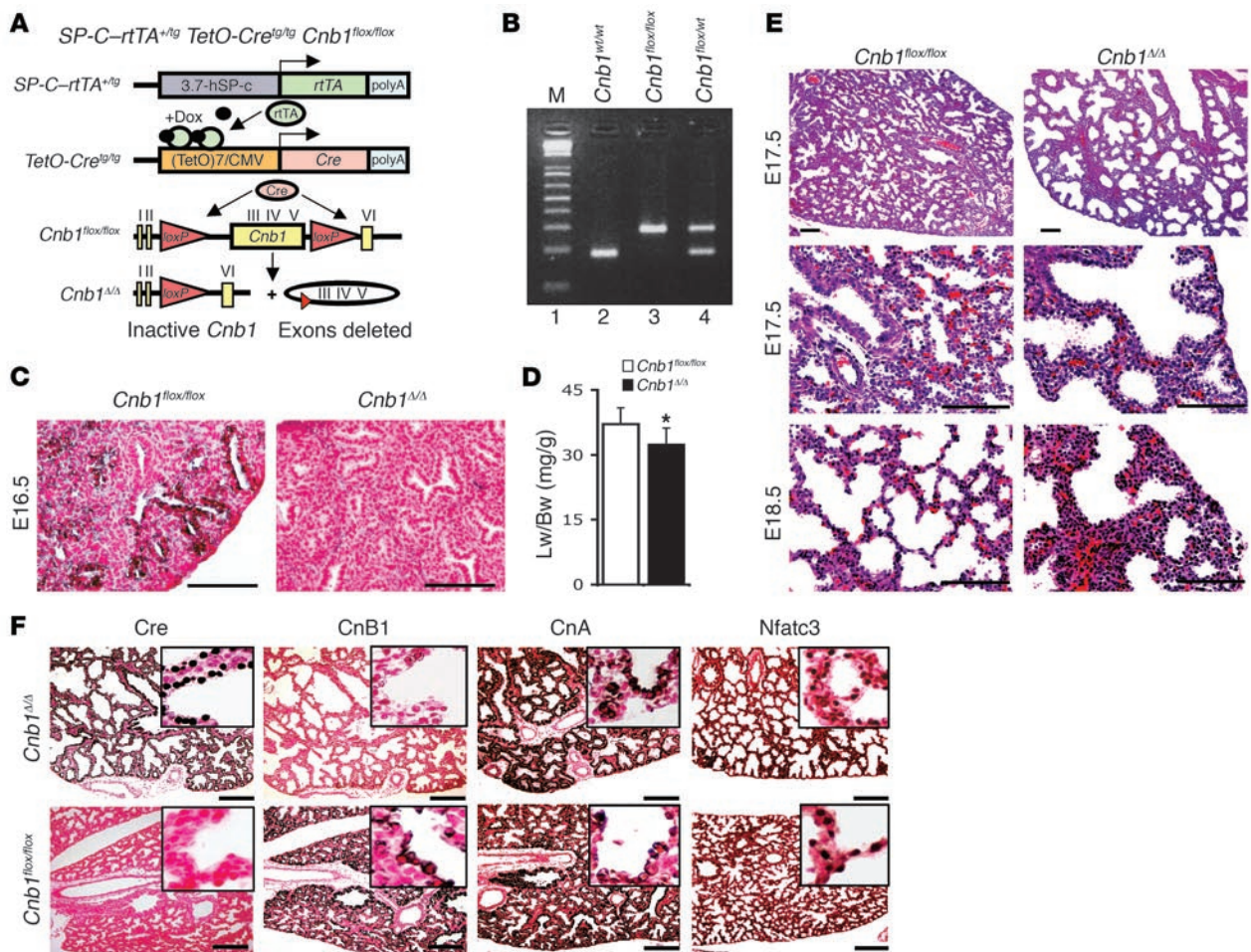
**Figure 2**
Deletion of *Cnb1* in the respiratory epithelium. (**A**) Deletion of *Cnb1* was achieved in mice bearing *loxP*-flanked exons III–V of *Cnb1* (*Cnb1flox/flox*). *Cnb1flox/flox* mice were mated to *SP-C–rtTA−/tg* mice and the *TetO-Cretg/tg* mice. Administration of doxycycline to dams deleted exon III, IV, and V of *Cnb1* in the respiratory epithelium of the embryos, termed *Cnb1Δ/Δ* mice. (**B**) PCR analysis of genomic DNA using primers flanking *loxP* sites in exon V identified *Cnb1wt/wt*, *Cnb1flox/flox*, and *Cnb1flox/wt* genotypes. M, DNA marker. (**C**) CnB1 staining was decreased or absent at E16.5 in *Cnb1Δ/Δ* mice. (**D**) Lung weight to body weight ratio (Lw/Bw) was decreased by 10% in *Cnb1Δ/Δ* mice (mean ± SD). *$P < 0.008$, unpaired 2-tailed Student's *t* test. (**E**) At E17.5 and E18.5, lung saccules of control *Cnb1flox/flox* mice were lined by squamous type I and cuboidal type II cells with thinning of the mesenchyme, while decreased sacculation and mesenchymal thickening was observed in *Cnb1Δ/Δ* mice. (**F**) In *Cnb1Δ/Δ* mice at E18.5, cells expressing Cre recombinase lacked CnB1 expression, while widespread CnB1 staining was observed in *Cnb1flox/flox* control littermates, which do not express Cre recombinase. Expression of Cre and the lack of CnB1 protein did not affect expression of CnA or Nfatc3 in *Cnb1Δ/Δ* mice. Scale bars: 100 μm (**C** and **E**); 200 μm (**F**). Magnification, ×100 (insets in **F**).

control lungs, demonstrating an extensive vascular bed with capillaries that were observed in close proximity to epithelial cells. In contrast, pulmonary vessels in *Cnb1Δ/Δ* mice were embedded in the thick mesenchyme that surrounded the immature saccules at E18.5, consistent with a delay in lung maturation. Formation of pulmonary arteries and bronchiolar smooth muscle was unaltered as assessed by NFATc1 and α-SMA staining (Supplemental Figure 1; supplemental material available online with this article; doi:10.1172/JCI27331DS1).

*Synthesis of pulmonary surfactant is dependent on the Cn/Nfat pathway.* RDS, a common cause of perinatal death in premature infants, is induced by the lack of pulmonary surfactant lipids and proteins (14). To determine whether respiratory failure in *Cnb1Δ/Δ* mice was associated with decreased surfactant production, surfactant proteins and lipids were assessed at E18.5. While pro–surfactant protein B (proSP-B)

and proSP-C were readily detected in control mice expressing *Cnb1*, both proteins were markedly decreased in the respiratory cells of *Cnb1Δ/Δ* mice (Figure 3A). *Sftpa*, *Sftpb*, and *Sftpc* mRNAs were significantly decreased (Figure 3, B and C). Likewise, surfactant protein levels — including those of SP-D — were significantly decreased in lung homogenates from *Cnb1Δ/Δ* mice (Figure 3D). Saturated phosphotidylcholine (Sat PC), a critical surfactant lipid, was decreased by approximately 40% (Figure 3E). Thus, CnB1 is required for normal perinatal surfactant synthesis. Staining of T1-α and aquaporin-5 were decreased after deletion of *Cnb1* (Figure 3F), consistent with the paucity of type I cell differentiation observed in histology. In contrast, staining for Foxj1 and CCSP, differentiation markers of conducting airway epithelial cells, was not altered (Figure 3F).

*Surfactant protein genes Sftpa, Sftpb, and Sftpc are direct transcriptional targets of the Cn/Nfat pathway.* Luciferase reporters containing
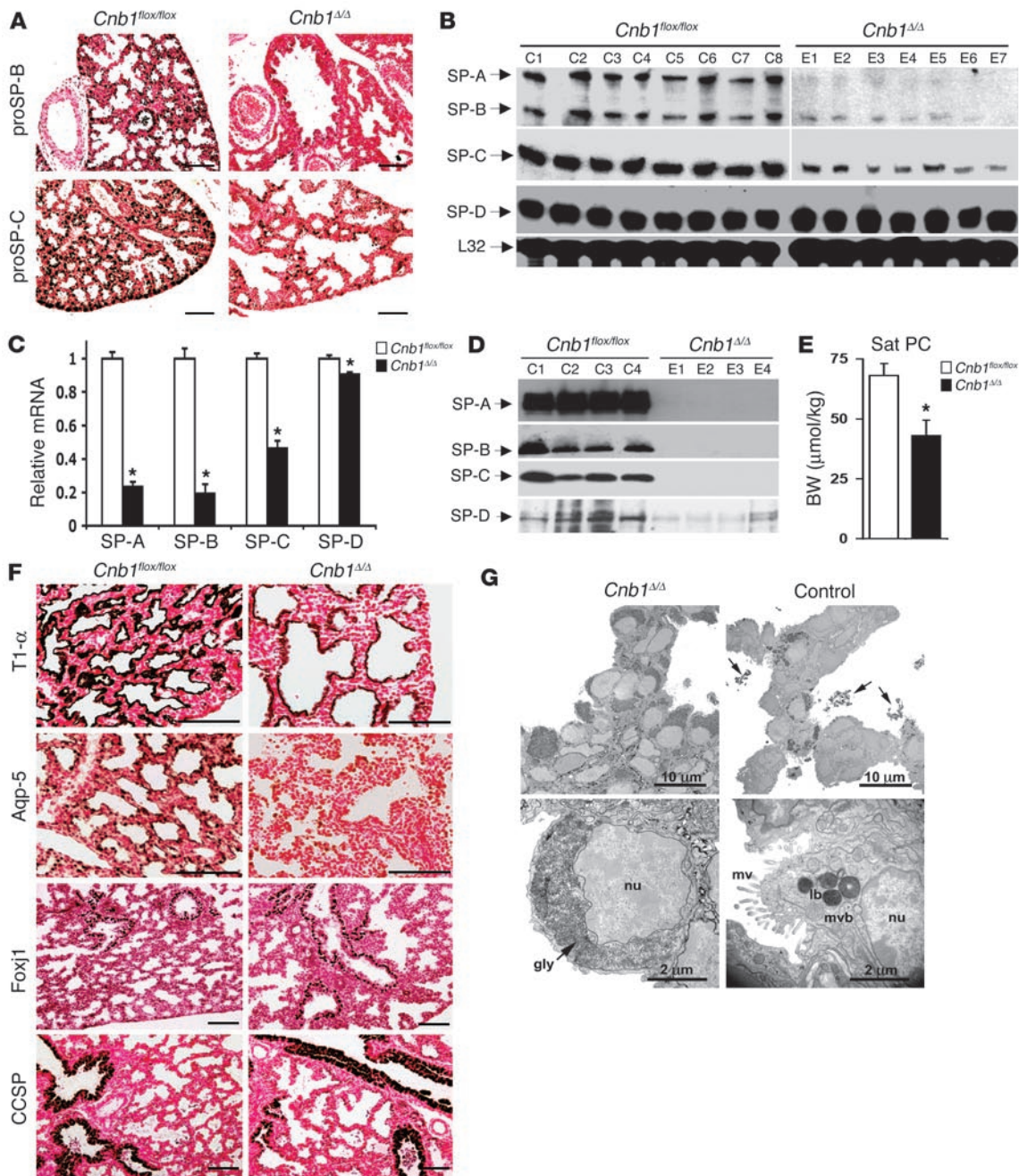
**Figure 3**
Defects in pulmonary surfactant synthesis and peripheral lung maturation in *Cnb1*^Δ/Δ mice. (**A**) proSP-B and proSP-C immunostaining was readily detected at E18.5 in control littermates, but was decreased in *Cnb1*^Δ/Δ mice. Scale bars: 100 μm. S1 nuclease analyses (**B** and **C**) and immunoblotting (**D**) of lung homogenates from *Cnb1*^Δ/Δ mice demonstratd decreased *Sftpa*, *Sftpb*, and *Sftpc* mRNA and protein. SP-D was decreased in *Cnb1*^Δ/Δ mice (**D**). (**E**) Sat PC was decreased by ~40% (mean ± SEM; *n* = 8–9 mice per genotype). *P < 0.05, unpaired 2-tailed Student's *t* test. (**F**) T1-α and aquaporin-5 (Aqp-5) staining was decreased, while Foxj1 and CCSP staining was unaltered. Scale bars: 100 μm. (**G**) Electron microscopy of fetal lungs from *Cnb1*^Δ/Δ and control mice at E18.5 demonstrated ultrastructural immaturity of the respiratory type II epithelial cells in the peripheral lung saccules. Alveolar epithelial cells lacked lamellar bodies and contained abundant glycogen (gly). Surfactant was absent from the luminal space. Lamellar bodies (lb), multivesicular bodies (mvb), decreased glycogen, microvilli (mv), and secreted surfactant (arrows) was observed in controls. nu, nucleus. Micrographs are representative of *n* = 3–4 separate mice per genotype.

5′ promoter regions of the *Sftpa*, *Sftpb*, and *Sftpc* genes (Supplemental Table 1) were activated when cotransfected with constitutively active Nfatc3 (CA-Nfatc3) in mouse lung epithelial cells (MLE-15 cells; Figure 4A). VIVIT, a potent Nfat-inhibitory peptide (15), inhib-

ited *Sftpa*, *Sftpb*, and *Sftpc* promoter activity (Figure 4B), suggesting direct transcription activation by Nfats. Cotransfection of Nfatc3 with TTF-1, an Nkx-2 homeodomain protein that is required for lung formation and gene expression in the respiratory epithelium,
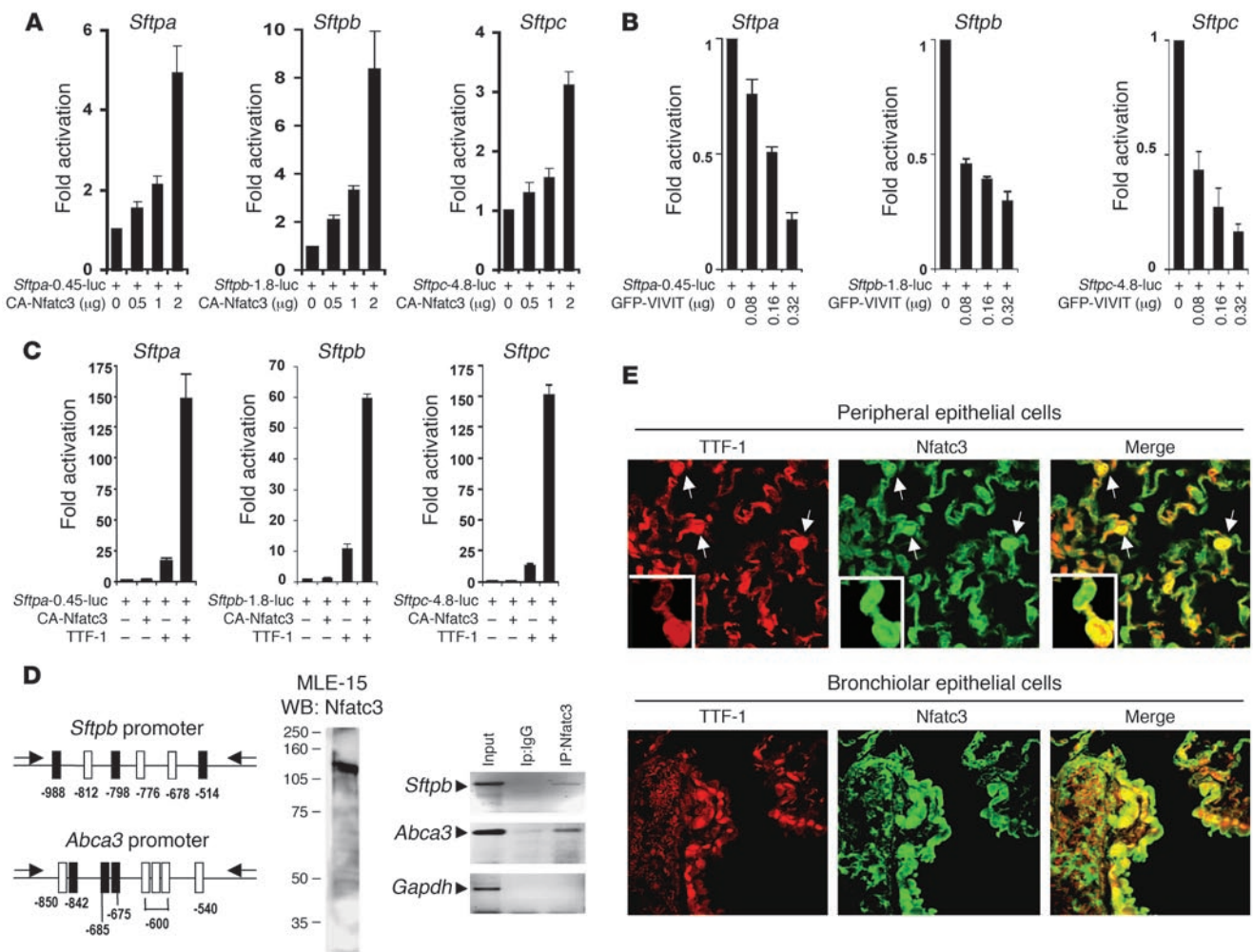
**Figure 4**

Synergistic activation of surfactant protein genes by Nfatc3 and TTF-1. (**A**) Nfatc3 activated *Sftpa*, *Sftpb*, and *Sftpc* promoters in MLE-15 cells. *Sftpa*-0.45-luc, *Sftpb*-1.8-luc, and *Sftpc*-4.8-luc (0.15 μg; see Supplemental Table 1) were cotransfected with CA-Nfatc3 (0, 0.5, 1, and 2 μg). (**B**) Expression of VIVIT (0, 0.08, 0.16, and 0.32 μg) inhibited transcription from *Sftpa*, *Sftpb*, and *Sftpc* promoter constructs (0.5 μg) in MLE-15 cells. (**C**) *Sftpa*, *Sftpb*, and *Sftpc* promoter constructs (1 μg) were synergistically activated by Nfatc3 (1 μg) and TTF-1 (1 μg) in HeLa cells. (**D**) ChIP assays on 5′-regulatory regions of *Sftpb* and *Abca3* gene (black boxes, GGAAA; white boxes, AGAAA) in MLE-15 cells, which express high levels of Nfatc3 identified direct binding of Nfatc3 in the chromatin. The proximal promoter of the mouse *Gapdh* gene served as a control. Input DNA was used as a PCR control. (**E**) Colocalization of Nfatc3 and TTF-1 immunostaining was observed in type II epithelial cells (white arrows) in peripheral lung and bronchiolar epithelial cells of mouse lungs, as demonstrated by yellow fluorescence in the merged images.

synergistically activated transcription from *Sftpa*, *Sftpb*, and *Sftpc* gene promoters in HeLa cells (Figure 4C). Direct binding of Nfatc3 to *Sftpb* promoter elements in chromatin was tested in MLE-15 cells, which express high levels of Nfatc3 (Figure 4D). Chromatin immunoprecipitation (ChIP) assay using DNA primers spanning the *Sftpb* 5′-regulatory region containing 3 adjacent consensus Nfat sites readily detected Nfatc3 binding in the chromatin of MLE-15 cells (Figure 4D). In contrast, Nfatc3 failed to bind *Gapdh* proximal promoter, implicating Nfatc3 as a direct transcriptional activator of *Sftpb*. Immunostaining of Nfatc3 and TTF-1 in adult mouse lungs demonstrated their colocalization in nuclei of alveolar and bronchiolar epithelial cells (Figure 4E). Thus Nfatc3 activated by Cn regulates surfactant protein gene transcription.

*Abca3 is a direct transcriptional target of the Cn/Nfat pathway*. In humans, mutations in *ABCA3* cause respiratory failure at birth

associated with surfactant deficiency (8). ABCA3 is present in the limiting membranes of lamellar bodies in type II epithelial cells (16) and plays a critical role in surfactant homeostasis. ABCA3 staining was markedly decreased in respiratory epithelial tubules of the peripheral lungs from $Cnb1^{\Delta/\Delta}$ mice at E18.5 (Figure 5A). The mechanism for transcriptional regulation of the *Abca3* gene in lung epithelial cells is unknown. To test the role of the Cn/Nfat pathway in transcriptional regulation of the *Abca3* gene, a 2.6-kb 5′ promoter region of the *Abca3* gene cloned into a luciferase reporter plasmid (Figure 5B and Supplemental Table 1) was cotransfected with CA-Nfatc3 in MLE-15 and HeLa cells. The *Abca3* promoter was activated by Nfatc3 in MLE-15 cells, and Nfatc3 and TTF-1 synergistically activated transcription from the *Abca3* promoter in HeLa cells, while VIVIT inhibited *Abca3* gene promoter activity in MLE-15 cells (Figure 5C). EMSAs were performed on 5 con-
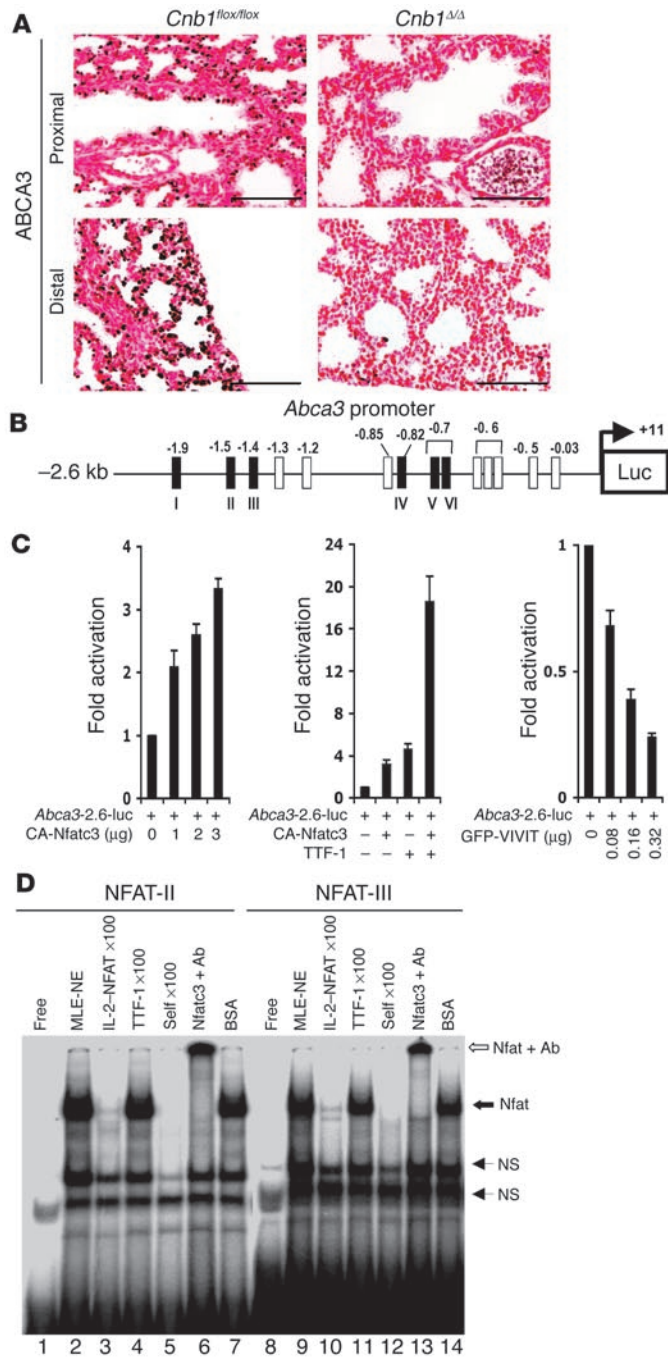
**Figure 5**
The *Abca3* gene is regulated by the Cn/Nfat pathway. (**A**) Immunostaining of ABCA3 was decreased in respiratory epithelial tubules of *Cnb1*$^{\Delta/\Delta}$ mice at E18.5. Scale bars: 100 μm. (**B**) Consensus Nfat sites were detected in the *Abca3* gene promoter. (**C**) The *Abca3* gene promoter was activated by Nfatc3 and TTF-1. CA-Nfatc3 expression vector (0, 1, 2, and 3 μg) cotransfected with *Abca3* promoter-luciferase constructs (1 μg; see Supplemental Table 1) in MLE-15 cells increased luciferase activity. TTF-1 (1 μg) and Nfatc3 (2 μg) expression synergistically activated the *Abca3* gene promoter (1 μg) in HeLa cells, and expression of VIVIT (0, 0.08, 0.16, and 0.32 μg) inhibited transcription from *Abca3* promoter constructs (0.25 μg) in MLE-15 cells. (**D**) EMSA with sites II and III of the *Abca3* promoter and proteins in MLE-15 cell nuclear extracts. DNA-protein complexes formed with each site that was competed by 100-fold excess of unlabeled self DNA (lanes 5 and 12) but not by 100-fold excess of TTF-1 consensus probe (lanes 4 and 11). A consensus Nfat site from the IL-2 promoter competed for complex formation with both sites (lanes 3 and 10). Antibodies to Nfatc3 supershifted DNA-protein complexes formed on both sites (lanes 6 and 13). Free DNA probes containing NFAT site (lanes 1 and 8). MLE–nuclear extract (MLE-NE) bound to NFAT site DNA probes (lanes 2 and 9). BSA incubated with MLE-NE and NFAT site DNA probes (lanes 7 and 14).

*Regulation of transcription factors Foxa1 and Foxa2 by the Cn/Nfat pathway.* The Foxa transcription factors play critical roles in lung morphogenesis and function (19, 20). Decreased staining of Foxa1 and Foxa2 in lungs from *Cnb1*$^{\Delta/\Delta}$ mice (Figure 6, B and E) indicated that the Cn/Nfat pathway was required for normal Foxa1/Foxa2 expression in late gestation. To determine whether Nfatc3 regulates the *Foxa1* and *Foxa2* genes, luciferase reporter plasmids containing 5′ promoter regions of *Foxa1* and *Foxa2* genes (Figure 6, A and F) were transiently transfected into HeLa and MLE-15 cells. Nfatc3 activated *Foxa1* and *Foxa2* promoters in both cell lines (Figure 6, C and G). Since Foxa2 and Foxa1 regulate genes required for lung function at birth, the effects of CnB1 deletion may be mediated in part by its effects on Foxa activity. Since the –3.4-kb *Foxa1* promoter contains 15 consensus Nfat binding sites as identified by MatInspector (version 7.0), EMSAs were performed on DNA elements with high matrix similarity (Supplemental Table 2). Sites IV, V, and VI (Figure 6D) bound Nfatc3 from MLE-15 nuclear extracts. An Nfat site competitor and unlabeled self DNA disrupted the DNA-protein complex, while a 100-fold molar excess of the TTF-1 probe did not affect the complex. Antibodies to Nfatc3 interfered with specific DNA-protein complex formation.

*Cn participates with TTF-1 in a transcriptional network during lung formation.* TTF-1, a homeodomain-containing member of the Nkx family of transcription factors, is expressed in the respiratory epithelial cells. TTF-1 regulates expression of surfactant protein genes, and mutations in *Titf1* leads to defects in lung formation and function (21). Since CnB1 is expressed in early embryonic lung buds at E11, we sought to determine whether lack of CnB1 influences *Titf1* expression and to explain, in part, the maturation defects seen in *Cnb1*$^{\Delta/\Delta}$ mice. The sites and intensity of TTF--1 staining were not altered in the lungs of *Cnb1*$^{\Delta/\Delta}$ mice, suggesting that CnB1 does not regulate TTF-1 expression (Figure 7A). Conversely, we tested whether TTF-1 regulates CnB1 and Nfatc3 expression. CnB1 staining was lacking in the respiratory epithelial cells in the lungs of TTF-1 null (*Titf1*$^{-/-}$) mice, while staining was observed in the surrounding mesenchyme (Figure 7B). In contrast,

sensus Nfat sites identified in the *Abca3* promoter. Sites II and III (Supplemental Table 2) bound proteins in MLE-15 cell nuclear extracts that were competed by 100-fold excess of unlabeled self DNA (Figure 5D) but not by 100-fold excess of a strong TTF-1 site (17), indicating that the protein bound specifically to Nfat sites. A strong Nfat site probe (18) inhibited DNA-protein complex formation at both sites, suggesting that these promoter elements bound Nfats. Antibodies to Nfatc3 supershifted DNA-protein complexes formed on both sites (Figure 5D). ChIP assay detected binding of Nfatc3 on *Abca3* promoter elements in the chromatin of MLE-15 cells (Figure 4D), supporting the concept that the Cn/Nfat pathway directly regulates *Abca3* gene transcription.
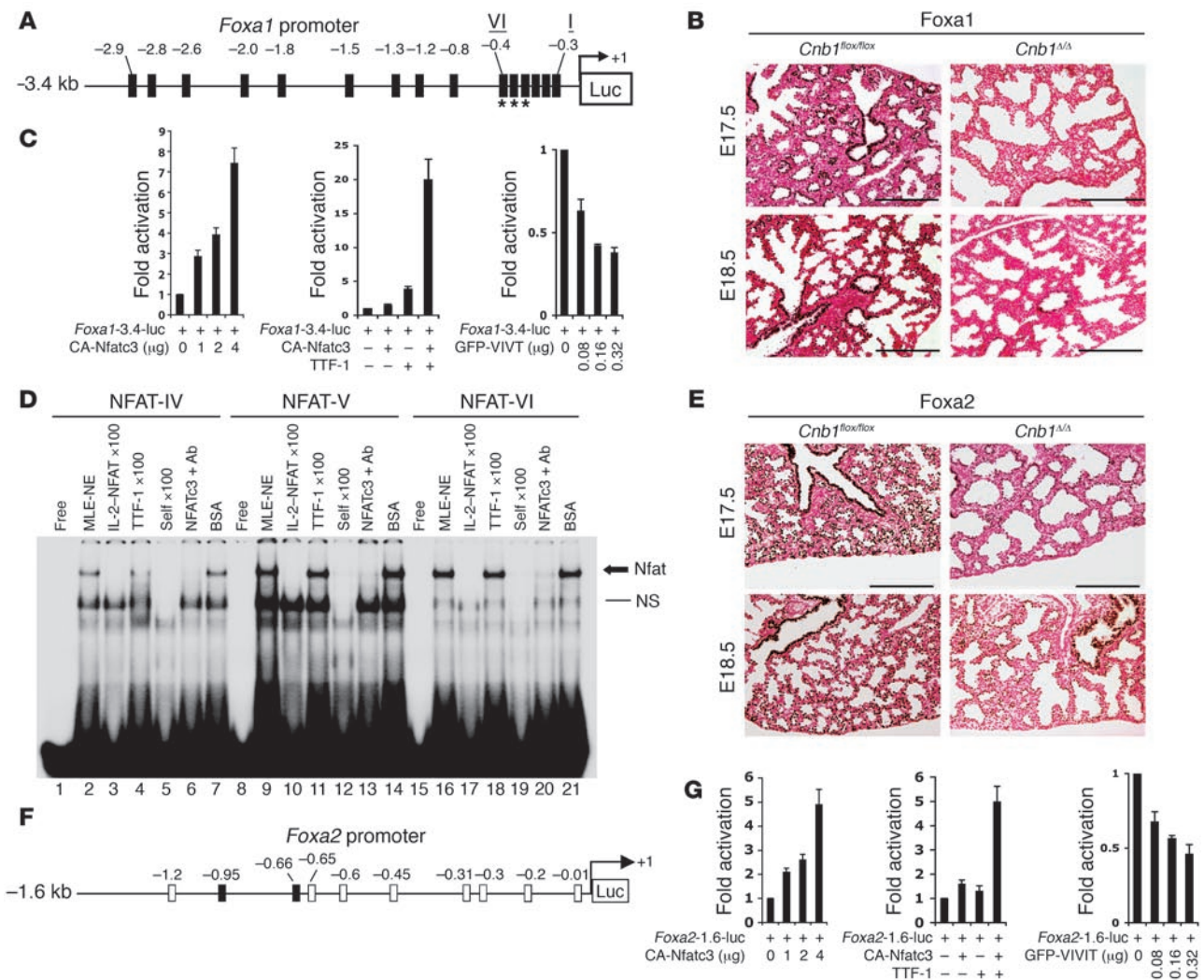
**Figure 6**
Cn influences *Foxa1* and *Foxa2* gene regulation. (**A**) Consensus Nfat site GGAAA in the *Foxa1* promoter. (**B**) Foxa1 staining was decreased in lungs from *Cnb1*^Δ/Δ mice at E17.5 and E18.5. Scale bars: 200 μm. (**C**) CA-Nfatc3 expression (0, 1, 2, and 4 μg) enhanced activity of *Foxa1* promoter-luciferase construct (0.08 μg; see Supplemental Table 1) in MLE-15 cells. TTF-1 (1 μg) and Nfatc3 (2 μg) synergistically activated the *Foxa1* promoter-luciferase construct (1 μg) in HeLa cells, while VIVIT expression vector (0, 0.08, 0.16, and 0.32 μg) inhibited activity of the *Foxa1* promoter-luciferase construct (0.165 μg) in MLE-15 cells. (**D**) Sites IV, V, and VI of *Foxa1* promoter bound Nfatc3 from nuclear extracts of MLE-15 cells. Complexes were competed by 100-fold molar excess of Nfat site from the IL-2 promoter (lanes 3, 10, and 17) and by unlabeled self DNA (lanes 5, 12, and 19) but not by TTF-1 site DNA (lanes 4, 11, and 18). Antibodies to Nfatc3 interfered with complex formation (lanes 6, 13, and 20). Free DNA probes containing NFAT site (lanes 1, 8, and 15). MLE-NE bound to DNA probes containing NFAT site (lanes 2, 9, and 16). BSA incubated with MLE-NE and DNA probes containing NFAT sites (lanes 7, 14, and 21). NS, nonspecific protein binding to DNA probes containing NFAT site. (**E**) Decreased Foxa2 immunostaining in lungs from *Cnb1*^Δ/Δ mice at E17.5 and E18.5. Scale bars: 200 μm. (**F**) Consensus Nfat sites (solid box: GGAAA; and open box: AGAAA) were identified in *Foxa2* promoter. (**G**) Nfatc3 activated the *Foxa2* promoter-luciferase construct (see Supplemental Table 1) in MLE-15 cells. Nfatc3 (2 μg) and TTF-1 (1 μg) synergistically activated the *Foxa2* promoter in HeLa cells. Expression of VIVIT inhibited transcription from the *Foxa2* promoter in MLE-15 cells.

intense Nfatc3 staining was evident in epithelial cells lining the lung saccules in *Titf1*^–/– mice at E16.5 and E18.5 (Figure 7B), suggesting that while TTF-1 regulated expression of CnB1, Nfatc3 expression was independent of TTF-1. Indeed, deletion of the *Cnb1* gene inhibited the nuclear localization of Nfatc3, while Nfatc3 and TTF-1 staining were colocalized in the nuclei of airway epithelial cells in lungs from normal *Cnb1*^flox/flox mice (Figure 7C).

*TTF-1 regulates Cnb1 expression.* A 755-bp 5′-regulatory region of the mouse *Cnb1* gene contained several adjacent TTF-1 and Nfat con-

sensus *cis* elements (Figure 8A). TTF-1 activated the *Cnb1* promoter in HeLa and MLE-15 cells. Expression of TTF-1 and Nfatc3 together synergistically increased *Cnb1* promoter activity in HeLa cells (Figure 8B), supporting the concept that TTF-1 and Nfatc3 interact and activate *Cnb1* gene transcription and consistent with the lack of CnB1 staining in the respiratory epithelial cells of *Titf1*^–/– mice.

*RNA microarray analysis of CnB1-regulated genes.* Microarray analysis of lung RNA from *Cnb1*^Δ/Δ and control mice identified 437 genes that were significantly altered (≥1.5-fold change): 243 mRNAs were
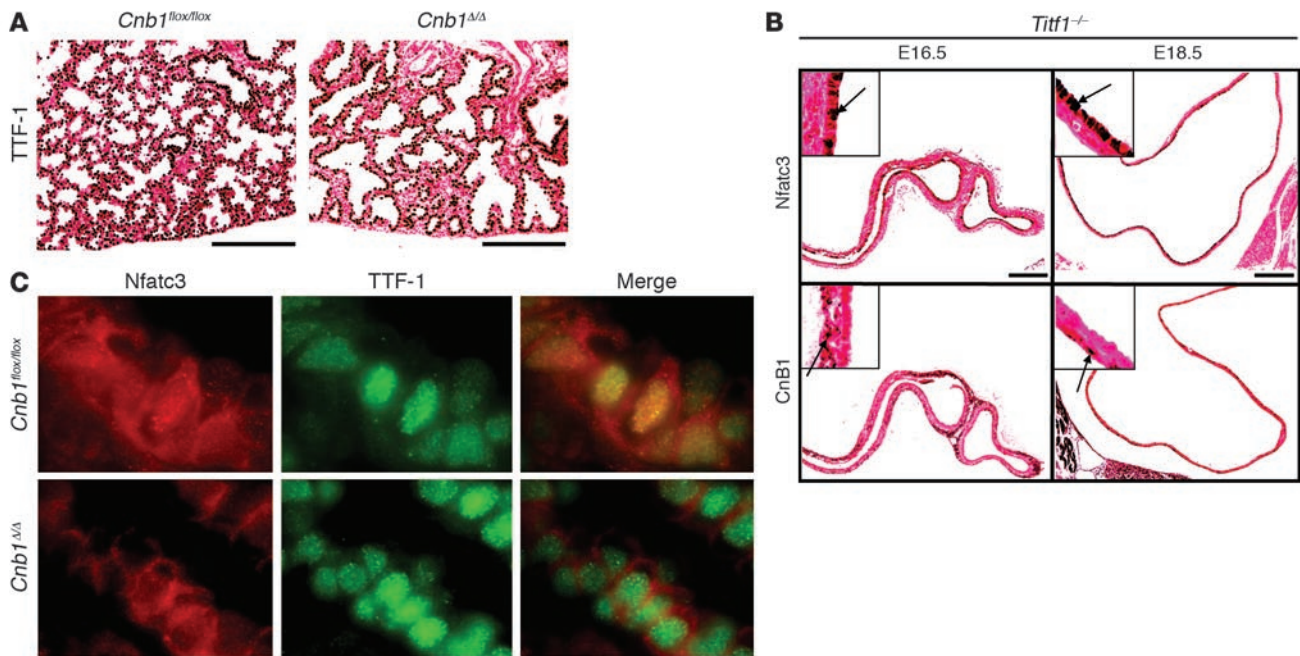
**Figure 7**
Role of TTF-1 in the regulation of CnB1 and Nfatc3 activity. (**A**) Neither sites nor intensity of TTF-1 staining was altered in lungs of $Cnb1^{\Delta/\Delta}$ mice at E18.5. (**B**) Nfatc3 staining was detected in respiratory epithelial cells of $Titf1^{-/-}$ mice (arrows), while CnB1 staining was lacking in respiratory epithelial cells, at E16.5 and E18.5. Note CnB1 staining in the mesenchyme (arrows). (**C**) Nuclear staining and colocalization of TTF-1 and Nfatc3 were observed in the lungs of $Cnb1^{flox/flox}$ mice at E18.5, as demonstrated by yellow fluorescence of the merged image. In contrast, staining of Nfatc3 and nuclear transcription factor TTF-1 were not colocalized in the nuclei of airway epithelial cells in $Cnb1^{\Delta/\Delta}$ mouse lungs. Scale bars: 200 μm. Magnification, ×40 (insets in **B**); ×100 (**C**).

increased, and 194 mRNAs were decreased (Supplemental Table 3). An additional filter was used (see Methods) to identify genes classified as involved in regulation of surface tension, respiratory air and gas exchange, lipid metabolism, and ion transport (See Supplemental Table 3 for gene ontology classification). Genes regulating lung function, including regulation of surface tension, respiratory air and gas exchange, lipid metabolism, and ion transport, were significantly decreased in the lungs of $Cnb1^{\Delta/\Delta}$ mice (Table 1). Pearson correlation analysis identified lung mRNAs that were similarly influenced after deletion of $Cnb1$ and $Foxa2$ and mutation of $Titf1$ in respiratory epithelial cells (Figure 9A and Supplemental Table 4). The list of genes differentially expressed in response to $Cnb1$ deletion correlated closely with those differentially expressed in $Foxa2^{\Delta/\Delta}$ mice ($r = 0.71$) and those in $Titf1$ phosphorylation mutant mice ($Titf1^{PM/PM}$ mice; $r = 0.58$).

Foxa2 and TTF-1 regulate expression of surfactant proteins and respiratory epithelial cell differentiation (21, 22). Comparison of lung mRNAs from $Cnb1^{\Delta/\Delta}$, $Foxa2^{\Delta/\Delta}$ (22), and $Titf1^{PM/PM}$ mice (21) demonstrated that a number of mRNAs were similarly influenced in each model, supporting the concept that their biological processes were shared (Figure 9A and Supplemental Table 4). Genes involved in the regulation of lung lipid homeostasis ($Lrp2$, $Sftpb$, $Abca3$, $Dlk1$, $Scd1$, and $Pon1$), fluid and electrolyte transport ($Aqp5$, $Clic5$, $Scnn1g$, and $Slc34a2$), and inflammation ($Sftpa1$, $Hc$, $Lyzs$, and $Lzp-s$) were decreased in response to the lung-selective deletion of $Cnb1$ or $Foxa2$ or mutation of phosphorylation sites in the $Titf1$ gene (see Supplemental Table 4 for a complete list of overlapping genes).

Deletion of $Cnb1$ altered expression of a number of genes regulating lipid synthesis. $Pla2g1b$ mRNA, which encodes a calcium-dependent phospholipase referred to as phosphatidylcholine 2-acylhydrolase (23), was increased approximately 3.7-fold in $Cnb1^{\Delta/\Delta}$ mice over that of $Cnb1^{flox/flox}$ mice. mRNA levels for $Aytl2$, a putative acetyltransferase that may regulate synthesis of Sat PC by addition of acyl groups, was decreased approximately 3.9-fold in $Cnb1^{\Delta/\Delta}$ mice compared with that of $Cnb1^{flox/flox}$ mice as assessed by real-time PCR, consistent with the RNA microarray data (Figure 9B).

## Discussion
Failed lung maturation at birth results in surfactant deficiency, causing respiratory distress in the perinatal period. The molecular mechanisms controlling maturation of the lung are poorly understood. The present study demonstrates that Cn/Nfat signaling was required for the structural, biochemical, and functional maturation of the lung prior to birth. Since $Cnb1$-null embryos die before lung formation (24), we used a conditional deletion strategy to ascertain the function of Cn in the developing respiratory epithelium. While the growth and branching of the lungs appeared to be normal in $Cnb1^{\Delta/\Delta}$ mice, structural abnormalities associated with delayed lung maturation were apparent in late gestation. Deletion of $Cnb1$ impaired sacculation and inhibited lung epithelial cell differentiation, consistent with a generalized arrest in lung maturation.

Expression of $Sftpb$ and $Abca3$ mRNA and protein as well as that of the surfactant lipids were markedly decreased in the lungs of $Cnb1^{\Delta/\Delta}$ mice. Since deletion of either $Sftpb$ or $ABCA3$ causes lethal respiratory failure at birth (8, 25), the lack of their expression is sufficient to explain respiratory failure in $Cnb1^{\Delta/\Delta}$ mice. The abnormalities in lung structure and decreased surfactant lipid synthesis are also likely factors contributing to poor respiratory function at birth.
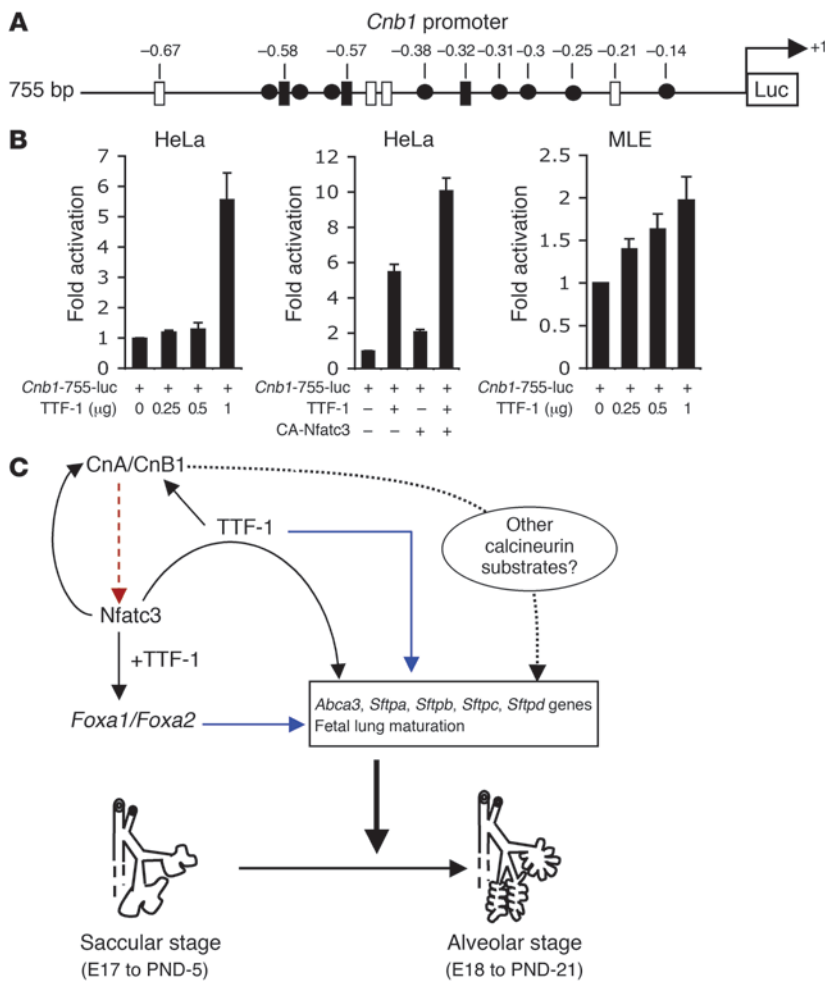
**Figure 8**
Regulation of *Cnb1* and its participation with TTF-1 in a transcriptional network during lung formation. (**A**) Consensus TTF-1 and Nfat sites were detected in the *Cnb1* proximal promoter. Black and white boxes represent Nfat sites (GGAAA and AGAAA, respectively); black circles represent TTF-1 sites. (**B**) The *Cnb1* gene promoter was activated by TTF-1 and Nfatc3. Cotransfection of TTF-1 expression vector (0, 0.25, 0.5, and 1 μg) with a fixed amount of *Cnb1*-755-luc (0.25 μg; a promoter-reporter construct containing −755 bps of 5′-upstream regulatory sequence of mouse *Cnb1* gene cloned into *Xho*I and *Hind*III site of pGL3 basic plasmid) increased luciferase activity in HeLa and MLE-15 cells. TTF-1 (0.5 μg) and Nfatc3 (0.5 μg) synergistically activated the *Cnb1* gene promoter in HeLa cells. (**C**) Proposed network of transcription factors — regulated by or interacting with the Cn/Nfat pathway — directing perinatal lung maturation. This maturation process begins in the saccular stage from E17 to postnatal day 5 (PND-5) and is completed at the end of the alveolar stage by PND-21 in mice. TTF-1 regulates CnB1 expression. CnB1 dephosphorylates and activates Nfatc3 (red dashed arrow). In turn, Nfatc3 (a) activates *Foxa1* and *Foxa2*; (b) synergistically interacts with TTF-1 to activate surfactant protein genes and *Abca3*; and (c) increases transcription of CnA required for its own activity (61). Foxa1, Foxa2, and TTF-1 are known to activate a number of shared target genes critical for lung function (blue arrows). Cn may also function via Nfat-independent pathways (dashed arrow).

The temporal and spatial expression of CnA, CnB1, and Nfatc3 in the developing lung epithelial cells is consistent with the concept that the Cn/Nfat pathway regulates critical genes involved in lung formation and function at birth. Nfatc3, a transcription factor and downstream effector of the Cn signaling pathway, enhanced transcription via direct binding and activation of target genes, including genes encoding surfactant proteins, providing evidence that disruption of the Cn/Nfat-mediated pathway is responsible, at least in part, for the observed phenotype after deletion of *Cnb1* in the lung.

RNA microarray analysis demonstrated that *Cnb1* regulated genes mediating innate host defense, electrolyte and fluid transport, and surfactant protein and lipid homeostasis, thus identifying a group of genes likely to play important roles in perinatal lung homeostasis. Since TTF-1 and Foxa2 regulate expression of surfactant proteins, and either mutations in *Titf1* (21) or deletion of *Foxa2* (22) delays lung maturation causing respiratory failure at birth, it seems likely that they share common transcriptional targets. This assumption is supported by the following findings: First, a number of common transcriptional target genes were identified that were influenced in *Cnb1*$^{\Delta/\Delta}$ and *Titf1*$^{PM/PM}$ mice in late gestation. Further, Nfatc3 and TTF-1 cooperatively activated transcription of a number of genes important during perinatal lung maturation, indicating that Nfatc3 and TTF-1 function together at a number of transcriptional targets during perinatal lung maturation. Second, Nfatc3 regulated Foxa2 transcription,

and RNA microarray analysis identified a common set of mRNAs influenced by both *Cnb1* and *Foxa2* deletion (22) with a high Pearson correlation, implying that the Cn/Nfat pathway appears to be upstream of Foxa2 activity, consequently sharing an overlapping set of transcriptional targets with *Cnb1*. Thus, the 3 transcription factors Nfatc3, Foxa2, and TTF-1 regulate a subset of genes crucial for perinatal lung maturation and function.

Nfats mediate gene transcription in immune and nonimmune cells (11). In our present studies, Nfatc3 directly bound and activated promoters of surfactant protein genes *Sftpa*, *Sftpb*, *Sftpc*, and *Abca3*. ChIP assays implicated direct binding of Nfatc3 to *Abca3* and *Sftpb* promoters. Because Nfats have low affinity for DNA binding, they engage in cooperative/synergistic interactions with other transcription factors, as seen with Nfat/AP1-DNA complex formation in immune cells (9, 26–28). Differences in the influence of NFATc3 on *Sftpd* mRNA expression in the developing lung seen in the *Cnb1*$^{\Delta/\Delta}$ mice and in in vitro transfection studies (12) may indicate transcription protein complex–dependent differences in gene regulation. In addition, Nfat forms heterodimers with transcriptional partners in other cellular processes including development of the nervous system, bone, cartilage, muscle, heart, skin, and fat tissues (29). For example, Nfat influences transcription by interacting with b-ZIP family members Maf, ATF2, ICER, C/EBP, and p21SNFT; zinc finger family members GATA-4, SP1, and EGR; helix-turn-helix proteins IRF-4 and Foxa2 (9, 30, 31); MADS-box protein MEF2 (32); and homeodomain-contain-

**Table 1**
Gene ontology analysis after *Cnb1* deletion in the lung epithelial cells

| Symbol | GenBank accession no. | Description | Ratio |
|---|---|---|---|
| *Sftpa1* | NM_023134 | Surfactant associated protein A1 | −43.09 |
| *Scd1* | NM_009127 | Stearol-Coenzyme A desaturase 1 | −25.22 |
| *Pon1* | NM_011134 | Paraoxonase 1 | −15.02 |
| *Aqp5* | NM_009701 | Aquaporin 5 | −13.60 |
| *Hc* | NM_010406 | Hemolytic complement | −5.02 |
| *Slc34a2* | NM_011402 | Solute carrier 34a2 | −4.92 |
| *Acoxl* | NM_028765 | Acyl-Coenzyme A oxidase-like | −4.2 |
| *Sftpb* | NM_147779 | Surfactant associated protein B | −2.57 |
| *Abca3* | NM_013855 | ABC1 member A3 | −2.33 |
| *Clic5* | NM_172621 | Chloride intracellular channel 5 | −2.17 |
| *Dlk1* | NM_010052 | Delta-like 1 homolog | −2.14 |
| *Lrp2* | XM_130308 | Low density lipoprotein receptor-related protein 2 | −2.04 |
| *Scnn1g* | NM_011326 | Sodium channel, nonvoltage-gated channel 1γ | −2.01 |
| *Slc12a5* | NM_020333 | Solute carrier family 12, member 5 | −1.90 |
| *Atp6v1c2* | NM_133699 | ATPase, H⁺-transporting, lysosomal V1 subunit C2 | −1.79 |
| *Cacna1c* | NM_009781 | Ca²⁺ channel, voltage-dependent, L type, alpha 1C subunit | −1.76 |
| *Slc7a10* | NM_017394 | Solute carrier family 7a, member 10 | −1.75 |
| *Sftpc* | NM_011359 | Surfactant associated protein C | −1.73 |
| *Scd2* | NM_009128 | Stearol-Coenzyme A desaturase 2 | −1.65 |
| *Abca13* | AY160971 | ABC1 member 13 | −1.55 |
| *Lyzs* | NM_017372 | Lysozyme | −1.54 |
| *Aqp1* | NM_007472 | Aquaporin 1 | −1.53 |

Expression of genes involved in lung maturation, lung function, and homeostasis — including regulation of surface tension, respiratory gas exchange, ion transport, fluid balance, lipid metabolism, and transport — were decreased. Note decrease in expression of *Abca3*, *Sftpb*, *Scd1*, and *Aqp5* mRNAs.

ing protein Oct-1 (33). Consistent with this property of NFAT interactions, C/EBPα plays important roles in perinatal lung maturation (34, 35). In the present study, Nfatc3 synergistically interacted with TTF-1, a homeodomain-containing Nkx-2 class of transcription factor. Since *Abca3*, *Foxa1/a2*, *SftpA*, *Sftpb*, and *Sftpc* are expressed in alveolar type II cells and MLE-15 cells, the posttranslational modifications required for protein-protein interactions with cofactors to form higher-order multiprotein transcriptional complexes would likely be present on Nfatc3 and TTF-1, regulating promoters of these genes. The synergistic interaction between Nfatc3 and TTF-1 is reiterated on a number of genes in respiratory epithelial cells, as previously demonstrated for the transcriptional regulation of the *Sftpd* gene (12).

While the present study supports the hypothesis for the role of Nfatc3 during perinatal lung maturation, it is also likely that abrogation of Cn activity may influence cellular processes via Nfat-independent mechanisms. Cn dephosphorylates diverse cellular proteins that directly influence cell functions including Bcl-2 and BAD, NO synthase, HSP70, GTPase dynamin 1, Elk-1, and cytoskeletal-associated proteins Gap43, Map-2, tau, and tubulin (36–42). Cn also modulates Ca²⁺ ion channels and IP3 and ryanodine receptors (43, 44). Thus Cn plays a central role in a variety of distinct cellular networks that influence signaling events independent of Nfats and may contribute in part to the lung phenotype of *Cnb1*$^{\Delta/\Delta}$ mice.

TTF-1 was required for the normal expression of CnB1 in the respiratory epithelium, and TTF-1 and Nfatc3 directly activated the *Cnb1* gene promoter. CnB1, in turn, influenced the expression of *Foxa1* and *Foxa2* via Nfatc3. Thus Foxa1, Foxa2, TTF-1, Nfatc3, and CnB1 interact in a complex transcriptional network that orchestrates the expression of groups of genes critical for the structural

and biochemical maturation of the lung required for respiration at birth (Figure 8C). Because TTF-1 phosphorylation is critical in regulating expression of genes involved in lung morphogenesis and surfactant protein production (21), it is plausible that distinct signaling events influence TTF-1 and Nfatc3 function at transcriptional and posttranslational levels, enabling them to synergize in the temporal, spatial, and cell-specific control of gene expression during perinatal lung maturation.

Taken together, our results suggest that under the influence of Cn signaling, Nfatc3 binds and activates the promoters of transcriptional targets mediating surfactant homeostasis, including *Abca3*, *Sftpa*, *Sftpb*, *Sftpc*, and *Sftpd*. Nfatc3 may directly interact with TTF-1 at transcriptional target sites. Cn activation is dependent on receptors present on the cell membrane (9, 32), providing a potential mechanism by which Nfatc3 function is influenced by external signals. The identification of an Cn/Nfat signaling axis in the respiratory epithelial cells presents opportunities to modulate this transcriptional program during perinatal adaptation that may provide a basis for the prevention or treatment of respiratory disease before and after birth.

## Methods

*Transgenic mouse lines.* CnA and CnB1 are both indispensable for the phosphatase activity of Cn. Thus deletion of *Cnb1*, the only isoform found in all tissues except the testis, is sufficient to eliminate Cn activity in the lung. Therefore, mice bearing *loxP*-flanked exons III–V of *Cnb1* (Figure 1A) were produced (45) and maintained as homozygotes in a mixed C57BL/6–SV129–FVB/N background. To achieve lung epithelium–specific deletion of the *Cnb1* gene, these mice were first mated to *SP-C–rtTA*$^{-/tg}$ mice and *TetO-Cre*$^{tg/tg}$ mice expressing Cre recombinase (13). Further backcrossings gave triple-transgenic mice harboring *SP-C–rtTA*$^{-/tg}$*TetO-Cre*$^{tg/tg}$*Cnb1*$^{flox/flox}$ alleles. Administration of doxycycline to dams from E0.5 to birth activated rtTA from the SP-C promoter in the lung epithelium and induced Cre (Cre recombinase), which deleted exons III–V of *Cnb1* in the lung epithelium and produced *Cnb1*$^{\Delta/\Delta}$ mice. *Cnb1*$^{flox/flox}$ littermates lacking either *rtTA* or *Cre* genes served as controls, herein termed *Cnb1*$^{flox/flox}$ mice. Further controls included mice expressing *rtTA* or *Cre* genes under the control of the SP-C promoter from the time of conception. In the absence of *loxP* alleles (*Cnb1*$^{flox/flox}$), rtTA- and Cre-expressing mice survived normally and without pulmonary abnormality. Genotypes were identified by PCR as previously described (13, 45). *Titf1*$^{-/-}$ mice (46), kindly provided by S. Kimura (NIH, Bethesda, Maryland, USA), were bred to obtain *Titf1*$^{-/-}$ lungs at E16.5 and E18.5. Lungs from *Titf1*$^{+/+}$ mice served as controls.

*Animal husbandry and doxycycline administration.* Animal studies were reviewed and approved by the Institutional Animal Care and Use Committee of Cincinnati Children's Hospital Research Foundation. Mice were housed in humidity- and temperature-controlled rooms on a 12-hour light/12-hour dark cycle with food and water ad libitum. There was no serologic or histologic evidence
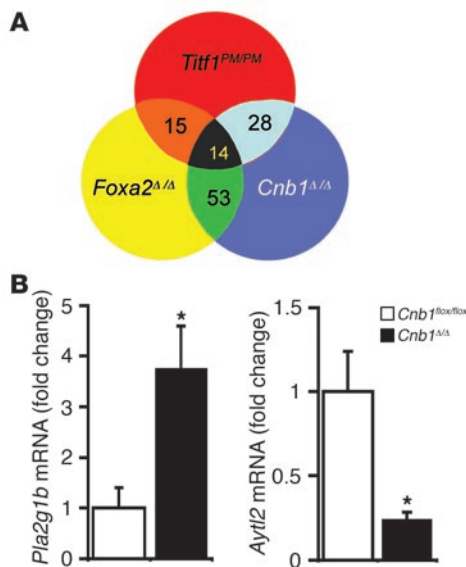
## Figure 9

RNA microarray analysis to identify CnB1 regulated genes. (**A**) Pearson correlation was used to identify lung mRNAs that were similarly influenced in $Foxa2^{\Delta/\Delta}$ and $Cnb1^{\Delta/\Delta}$ mice ($r = 0.71$) as well as in $Titf1^{PM/PM}$ and $Cnb1^{\Delta/\Delta}$ mice ($r = 0.58$). (**B**) Real-time RT-PCR measurement of mRNAs for $Pla2g1b$, $Aytl2$, and $\beta$-actin. Data were normalized to $\beta$-actin mRNA, and values from control lung mRNA were set to unity to calculate the fold change in mRNA after deletion of $Cnb1$. $Pla2g1b$ mRNA was increased ~3.7-fold, while $Aytl2$ mRNA decreased by ~3.9-fold ($n = 3$ per group) in $Cnb1^{\Delta/\Delta}$ (black bars) as compared with $Cnb1^{flox/flox}$ (white bars) lung tissue at E18. Values (mean ± SD) were obtained from 3 independent experiments for each sample. *$P < 0.05$, unpaired 2-tailed Student's $t$ test.

of either pulmonary pathogens or infections in sentinel mouse colonies. Gestation was dated E0.5 by vaginal plug. Dams were maintained on doxycycline in food (25 mg/g; Harlan Teklad) from E0.5 were and killed by injection of anesthetic to obtain embryos.

*Histology and immunohistochemistry.* Fetal and adult lungs were prepared as previously described (47). Antibodies used were as follows: CnA (diluted 1:200, anti-mouse rabbit polyclonal; Chemicon International AB-1695); CnB1 (diluted 1:700, anti-mouse rabbit polyclonal, PA-3025; Affinity Bio-Reagents); Cre (diluted 1:20, K; Novagen, EMD Biosciences); Nfatc3 (diluted 1:100, mouse monoclonal), F-1, SC-8405X; Santa Cruz Biotechnology Inc.); Nfatc1 (diluted 1:200, mouse monoclonal, SC-7294X; Santa Cruz Biotechnology Inc.); proSP-C (diluted 1:1,500, rabbit polyclonal, AB-3428; Chemicon International); CCSP (diluted 1:1,000, rabbit polyclonal, kindly provided by B. Stripp, University of Pittsburgh, Pittsburgh, Pennsylvania, USA); proSP-B (diluted 1:1,500, rabbit polyclonal, generated in the lab of J.A. Whitsett); Fox J1 (diluted 1:5,000, anti-mouse guinea pig polyclonal, generated in this lab); T1-α (diluted 1:1,000 anti-mouse hamster polyclonal 8.1.1, University of Iowa Hybridoma bank); aquaporin-5 (diluted 1:20, kindly provided by A. Menon, University of Cincinnati Medical Center, Cincinnati, Ohio, USA); TTF-1 (diluted 1:3,000, rabbit polyclonal, kindly provided by R. DiLauro, Laboratory of Biochemistry and Molecular Biology, Stazione Zoologica, Naples, Italy); Foxa1 and Foxa2 (both diluted 1:16,000, generated in this lab; ref. 48); ABCA3 (diluted 1:500, anti-mouse rabbit polyclonal, kindly provided by T. Weaver, University of Cincinnati, Cincinnati, Ohio, USA); and α-SMA (diluted 1:10,000; Sigma-Aldrich 1a4). Immunostaining and electron microscopy procedures were as previously described (47, 49). For immunofluorescence studies a 10-fold higher titer of antibodies was used. All results shown are representative of at least 3–4 triple-transgenic offspring that were compared with control littermates.

*Cell culture, transfection, and transcriptional reporter assays.* HeLa cells were cultured in DMEM with 10% FBS. MLE-15 cells were cultured as previously described (50). Transfection and reporter assays were carried out as previously described (12).

*EMSA.* Nuclear extracts from MLE-15 cells were made as previously described (12). EMSA probes (Supplemental Table 2) were derived from the 5′ promoter region of *Abca3* and *Foxa1* genes containing consensus Nfat sites (core similarity, 1.0; matrix similarity, ≥0.85; MatInspector 7.0 Software; Genomatix). EMSAs and antibody supershift assays were performed as previously described (12). Unlabeled double-stranded DNA competitors

with a strong TTF-1 binding site from the rat thyroglobulin gene (*rTg*; ref. 17) and a strong Nfat binding site from the IL-2 promoter (18) were added at 100-fold molar excess. The gels were dried and autoradiographed.

*Surfactant lipid and protein analysis.* Lungs were harvested at E18.5. The left lobe was homogenized in 0.9% NaCl. Sat PC was extracted using the osmium tetroxide ($OsO_4$) method (51) followed by phosphorous measurement (52). For SP-B and SP-C immunoblots, equal aliquots of the left lung homogenates were loaded on a 10%–20% Tricine SDS-PAGE (Invitrogen) and electroblotted to nitrocellulose membranes (0.1 μm; MidSci). Blots were blocked with 5% nonfat dry milk in TBST (10 mM Tris, pH 8, 150 mM NaCl, 0.1% Tween 20) and incubated with antibodies against human SP-B and SP-C (Chemicon International). To estimate SP-A and SP-D content, proteins from lung homogenates were resolved on 10%–20% Tris Glycine SDS-PAGE and electroblotted to nitrocellulose membranes (0.45 μm; Bio-Rad). For immunoblot analysis, guinea pig anti-rat SP-A or rabbit anti-mouse SP-D antibodies (53) were used. Secondary antibodies used were as follows: SP-A (goat anti-guinea pig IgG–peroxidase conjugate; Sigma-Aldrich); SP-B, SP-C, and SP-D (goat anti-rabbit heavy- and light-chain–peroxidase conjugate; Calbiochem, EMD Biosciences). MLE-15 whole-cell lysates run on 10%–20% Tris Glycine SDS-PAGE detected Nfatc3 by immunoblotting using mouse monoclonal antibody (F-1, SC-8405X; diluted 1:5,000, Santa Cruz Biotechnology Inc.), followed by anti-mouse goat IgG (Calbiochem, EMD Biosciences). Blots were developed by chemiluminescence (Pierce Biotechnology) and autoradiographed.

*RNA isolation and S1 nuclease analysis.* Lung RNA prepared by TRIZOL method (Invitrogen) was measured by UV absorbance and used for microarray and S1 analyses as previously described (21). Relative changes in SP-A, SP-B, SP-C, and SP-D mRNAs were assessed by S1 nuclease assays with ribosomal protein L32 as an internal control (54) using a phosphorimager.

*RNA microarray analysis.* Lung cRNA was hybridized to the murine genome MOE430 chips (Affymetrix) according to the manufacturer's protocol. Affymetrix Microarray Suite 5.0 was used to scan and quantitate the gene chips under default settings. Normalization was performed using the robust multichip average model (54, 56). Data were analyzed using Genespring 7.2 (Silicon Genetics). A volcano plot was used to identify significance (negative log of *P* values from Welch's approximate *t* test on *y* axis) and magnitude of change (log2 of fold change on the *x* axis) in the expression of a set of genes between $Cnb1^{\Delta/\Delta}$ mice and control littermates. The selection criteria included a *P* value of 0.05 or less by 2-tailed Student's *t* test, false discovery rate (FDR) of no more than 10% (57), and fold change of at least 1.5. Differentially expressed genes were subjected to an additional filter and classified according to Gene Ontology classification on Biological Process using the publicly available web-based tool David (58). The Fisher exact test was used to calculate the probability of each gene ontology category that was overrepresented in the selected list, using the entire MOE430 mouse genome as a reference data set. Pearson correlation identified lung mRNAs that were

similarly influenced after deletion of *Foxa2* and *Cnb1* and mutation of *Titf1* in respiratory epithelial cells. Differentially expressed genes ($P < 0.05$, 2-tailed Student's *t* test; fold change, >1.5) were compared, and correlations of transcript changes among 3 microarray experiments were measured.

*ChIP assays.* ChIP assays were performed as described previously by Li et al. (59), with modifications. Nfatc3 expression vector was transfected into about 80% confluent MLE-15 cells on 2 150-mm dishes using Lipofectamine 2000 (Invitrogen). After 24 hours, cells were treated with 1% formaldehyde for 10 minutes at 24°C, crosslinking was terminated by 0.125 M glycine, and cells were then washed in cold PBS and centrifuged to collect pellets that were resuspended in 10 ml lysis buffer 1 (50 mM HEPES-KOH, pH 7.9; 140 mM NaCl; 1 mM EDTA; 10% glycerol; 0.5% IGEPAL CA-630 from Sigma-Aldrich; 0.25% Triton X-100; and protease inhibitor cocktail from Roche Diagnostics) and incubated overnight at 4°C on a neutator. The lysates were collected by centrifugation, resuspended in 10 ml lysis buffer 2 (10 mM Tris-HCl, pH 7.8; 200 mM NaCl; 1 mM EDTA; 0.5 mM EGTA; 1% SDS; and protease inhibitors from Roche Diagnostics), and incubated for 10 minutes at 24°C on a neutator. After centrifugation, the pellet was resuspended in 2 ml lysis buffer 3 (10 mM Tris-HCl, pH 7.8; 1 mM EDTA; 0.5 mM EGTA; and protease inhibitors from Roche Diagnostics) and sonicated using Micro-Ultrasonic Cell Disrupter (Kimble-Kontes) to shear DNA (~500 bps). Sarkosyl was added to a final concentration of 0.5% for 10 minutes at 24°C and centrifuged. The soluble chromatin was mixed with magnetic beads (Dynal) precoupled with the Nfatc3 antibody (Santa Cruz Biotechnology Inc.) at 4°C overnight. The beads were washed 5 times with 1 ml RIPA buffer (50 mM HEPES-KOH, pH 7.9; 1 mM EDTA; 0.7% DOC; 1% IGEPAL CA-630; 0.5 M LiCl; and protease inhibitors from Roche Diagnostics) and once with 1 ml TE buffer and were resuspended in 50 μl elution buffer (50 mM Tris-HCl, pH 7.8; 10 mM EDTA; and 1% SDS). Precipitated chromatin was eluted at 65°C for 10 minutes and incubated at 65°C overnight to reverse the crosslinks. The next day, the DNA was phenol extracted, precipitated with ethanol, and dissolved in 50 μl of 10 mM Tris-HCl (pH 8.0). PCRs were performed using primers spanning the 5′-regulatory regions of the *Sftpb*, *Abca3*, and *Gapdh* genes (Supplemental Table 1). Reaction conditions were as follows: 95°C for 5 minutes; 35 cycles of amplification at 95°C for 30 seconds, then 55°C (*Sftpb* and *Abca3*) or 53°C (*Gapdh*) for 30 seconds; followed by 72°C for 30 seconds as an extension reaction. The products were analyzed by agarose gel electrophoresis.

*Real-time RT-PCR assays.* Lung RNA was prepared as described above. cDNA was synthesized from 5 μg total RNA as previously described (12) and analyzed by real-time PCR for *Pla2g1b* and *Aytl2* mRNA on a SmartCycler (Cepheid) as previously described (60). The values were normalized to β-*actin* values in each sample. Reaction conditions were as follows: 95°C for 150 seconds; 40 cycles of amplification at 95°C for 10 seconds, then 60°C (*Aytl2*) or 57.5°C (*Pla2g1b* and β-*actin*) for 10 seconds; followed by 72°C for 20–25 seconds (see primers in Supplemental Table 2).

*Statistics.* Quantitative results for gene activation analysis represent the average of at least 3 transfection experiments performed in duplicate ($n = 6$) and depicted as mean ± SD for data shown in Figures 4–6 and 8. For quantitative RNA and Sat PC analysis represented in Figure 3, statistical differences were determined using unpaired 2-tailed Student's *t* tests. Mean ± SEM values are shown ($n = 7$–9 mice per genotype). A *P* value of less than 0.05 was considered to be significant throughout this article.

Address correspondence to: Vrushank Davé, Division of Pulmonary Biology, Room 4403, Cincinnati Children's Hospital Research Foundation, University of Cincinnati Medical Center, 3333 Burnet Avenue, Cincinnati, Ohio 45229, USA. Phone: (513) 636-3323 or (513) 636-8410; Fax: (513) 636-7868; E-mail: davev0@cchmc.org.

1. Burri, P.H. 1984. Fetal and postnatal development of the lung. *Annu. Rev. Physiol.* **46**:617–628.
2. Williams, M.C., and Mason, R.J. 1977. Development of the type II cell in the fetal rat lung. *Am. Rev. Respir. Dis.* **115**:37–47.
3. Jobe, A.H., and Bancalari, E. 2001. Bronchopulmonary dysplasia. *Am. J. Respir. Crit. Care Med.* **163**:1723–1729.
4. Warburton, D., and Bellusci, S. 2004. The molecular genetics of lung morphogenesis and injury repair. *Paediatr. Respir. Rev.* **5**(Suppl. A):S283–S287.
5. Whitsett, J.A., Wert, S.E., and Trapnell, B.C. 2004. Genetic disorders influencing lung formation and function at birth. *Hum. Mol. Genet.* **13**:R207–R215.
6. Liggins, G.C., and Howie, R.N. 1972. A controlled trial of antepartum glucocorticoid treatment for prevention of the respiratory distress syndrome in premature infants. *Pediatrics.* **50**:515–525.
7. Shah, V., Ohlsson, A., Halliday, H.L., and Dunn, M.S. 2000. Early administration of inhaled corticosteroids for preventing chronic lung disease in ventilated very low birth weight preterm neonates. *Cochrane Database Syst. Rev.* **2**:CD001969.
8. Shulenin, S., et al. 2004. ABCA3 gene mutations in newborns with fatal surfactant deficiency. *N. Engl. J. Med.* **350**:1296–1303.
9. Hogan, P.G., Chen, L., Nardone, J., and Rao, A. 2003. Transcriptional regulation by calcium, calcineurin, and NFAT. *Genes Dev.* **17**:2205–2232.
10. Rusnak, F., and Mertz, P. 2000. Calcineurin: form and function. *Physiol. Rev.* **80**:1483–1521.
11. Graef, I.A., Chen, F., and Crabtree, G.R. 2001. NFAT signaling in vertebrate development. *Curr. Opin. Genet. Dev.* **11**:505–512.
12. Dave, V., Childs, T., and Whitsett, J.A. 2004. Nuclear factor of activated T cells regulates transcription of the surfactant protein D gene (Sftpd) via direct interaction with thyroid transcription factor-1 in lung epithelial cells. *J. Biol. Chem.* **279**:34578–34588.
13. Perl, A.K., Tichelaar, J.W., and Whitsett, J.A. 2002. Conditional gene expression in the respiratory epithelium of the mouse. *Transgenic Res.* **11**:21–29.
14. Whitsett, J.A., and Weaver, T.E. 2002. Hydrophobic surfactant proteins in lung function and disease. *N. Engl. J. Med.* **347**:2141–2148.
15. Aramburu, J., et al. 1999. Affinity-driven peptide selection of an NFAT inhibitor more selective than cyclosporin A. *Science.* **285**:2129–2133.
16. Mulugeta, S., et al. 2002. Identification of LBM180, a lamellar body limiting membrane protein of alveolar type II cells, as the ABC transporter protein ABCA3. *J. Biol. Chem.* **277**:22147–22155.
17. Civitareale, D., Lonigro, R., Sinclair, A.J., and Di Lauro, R. 1989. A thyroid-specific nuclear protein essential for tissue-specific expression of the thyroglobulin promoter. *EMBO J.* **8**:2537–2542.
18. Molkentin, J.D., et al. 1998. A calcineurin-dependent transcriptional pathway for cardiac hypertrophy. *Cell.* **93**:215–228.
19. Wan, H., et al. 2005. Compensatory roles of Foxa1 and Foxa2 during lung morphogenesis. *J. Biol. Chem.* **280**:13809–13816.
20. Wan, H., et al. 2004. Foxa2 regulates alveolarization and goblet cell hyperplasia. *Development.* **131**:953–964.
21. DeFelice, M., et al. 2003. TTF-1 phosphorylation is required for peripheral lung morphogenesis, perinatal survival, and tissue-specific gene expression. *J. Biol. Chem.* **278**:35574–35583.
22. Wan, H., et al. 2004. Foxa2 is required for transition to air breathing at birth. *Proc. Natl. Acad. Sci. U. S. A.* **101**:14449–14454.
23. Seilhamer, J.J., Randall, T.L., Yamanaka, M., and Johnson, L.K. 1986. Pancreatic phospholipase A2: isolation of the human gene and cDNAs from porcine pancreas and human lung. *DNA.* **5**:519–527.
24. Graef, I.A., Chen, F., Chen, L., Kuo, A., and Crabtree, G.R. 2001. Signals transduced by Ca(2+)/calcineurin and NFATc3/c4 pattern the developing vasculature. *Cell.* **105**:863–875.
25. Clark, J.C., et al. 1995. Targeted disruption of the surfactant protein B gene disrupts surfactant homeostasis, causing respiratory failure in newborn mice. *Proc. Natl. Acad. Sci. U. S. A.* **92**:7794–7798.
26. Crabtree, G.R. 1989. Contingent genetic regulatory events in T lymphocyte activation. *Science.* **243**:355–361.
27. Flanagan, W.M., Corthesy, B., Bram, R.J., and Crabtree, G.R. 1991. Nuclear association of a T-cell transcription factor blocked by FK-506 and cyclosporin A.

*Nature.* **352**:803–807.

28. Chen, L., Glover, J.N., Hogan, P.G., Rao, A., and Harrison, S.C. 1998. Structure of the DNA-binding domains from NFAT, Fos and Jun bound specifically to DNA. *Nature.* **392**:42–48.

29. Horsley, V., and Pavlath, G.K. 2002. NFAT: ubiquitous regulator of cell differentiation and adaptation. *J. Cell Biol.* **156**:771–774.

30. Lawrence, M.C., McGlynn, K., Park, B.H., and Cobb, M.H. 2005. ERK1/2-dependent activation of transcription factors required for acute and chronic effects of glucose on the insulin gene promoter. *J. Biol. Chem.* **280**:26751–26759.

31. Yang, T.T., and Chow, C.W. 2003. Transcription cooperation by NFAT.C/EBP composite enhancer complex. *J. Biol. Chem.* **278**:15874–15885.

32. Crabtree, G.R., and Olson, E.N. 2002. NFAT signaling: choreographing the social lives of cells. *Cell.* **109**(Suppl.):S67–S79.

33. Bert, A.G., Burrows, J., Hawwari, A., Vadas, M.A., and Cockerill, P.N. 2000. Reconstitution of T cell-specific transcription directed by composite NFAT/Oct elements. *J. Immunol.* **165**:5646–5655.

34. Basseres, D.S., et al. 2006. Respiratory failure due to differentiation arrest and expansion of alveolar cells following lung-specific loss of the transcription factor C/EBPalpha in mice. *Mol. Cell. Biol.* **26**:1109–1123.

35. Martis, P.C., et al. 2006. C/EBPalpha is required for lung maturation at birth. *Development.* **133**:1155–1164.

36. Wang, H.G., et al. 1999. Ca2+-induced apoptosis through calcineurin dephosphorylation of BAD. *Science.* **284**:339–343.

37. Dawson, T.M., et al. 1993. Immunosuppressant FK506 enhances phosphorylation of nitric oxide synthase and protects against glutamate neurotoxicity. *Proc. Natl. Acad. Sci. U. S. A.* **90**:9808–9812.

38. Lakshmikuttyamma, A., Selvakumar, P., and Sharma, R.K. 2006. Interaction between heat shock protein 70 kDa and calcineurin in cardiovascular systems. *Int. J. Mol. Med.* **17**:419–423.

39. Liu, J.P., Sim, A.T., and Robinson, P.J. 1994. Calcineurin inhibition of dynamin I GTPase activity coupled to nerve terminal depolarization. *Science.* **265**:970–973.

40. Sugimoto, T., Stewart, S., and Guan, K.L. 1997. The calcium/calmodulin-dependent protein phosphatase calcineurin is the major Elk-1 phosphatase. *J. Biol. Chem.* **272**:29415–29418.

41. Bolsover, S.R. 2005. Calcium signalling in growth cone migration. *Cell Calcium.* **37**:395–402.

42. Goto, S., et al. 1985. Dephosphorylation of microtubule-associated protein 2, tau factor, and tubulin by calcineurin. *J. Neurochem.* **45**:276–283.

43. Lieberman, D.N., and Mody, I. 1994. Regulation of NMDA channel function by endogenous Ca(2+)-dependent phosphatase. *Nature.* **369**:235–239.

44. MacMillan, D., Currie, S., Bradley, K.N., Muir, T.C., and McCarron, J.G. 2005. In smooth muscle, FK506-binding protein modulates IP3 receptor-evoked Ca2+ release by mTOR and calcineurin. *J. Cell Sci.* **118**:5443–5451.

45. Neilson, J.R., Winslow, M.M., Hur, E.M., and Crabtree, G.R. 2004. Calcineurin B1 is essential for positive but not negative selection during thymocyte development. *Immunity.* **20**:255–266.

46. Kimura, S., et al. 1996. The T/ebp null mouse: thyroid-specific enhancer-binding protein is essential for the organogenesis of the thyroid, lung, ventral forebrain, and pituitary. *Genes Dev.* **10**:60–69.

47. Wert, S.E., et al. 2000. Increased metalloproteinase activity, oxidant production, and emphysema in surfactant protein D gene-inactivated mice. *Proc. Natl. Acad. Sci. U. S. A.* **97**:5972–5977.

48. Besnard, V., Wert, S.E., Hull, W.M., and Whitsett, J.A. 2004. Immunohistochemical localization of Foxa1 and Foxa2 in mouse embryos and adult tissues. *Gene Expr. Patterns.* **5**:193–208.

49. Zeng, X., Wert, S.E., Federici, R., Peters, K.G., and Whitsett, J.A. 1998. VEGF enhances pulmonary vasculogenesis and disrupts lung morphogenesis in vivo. *Dev. Dyn.* **211**:215–227.

50. Wikenheiser, K.A., et al. 1993. Production of immortalized distal respiratory epithelial cell lines from surfactant protein C/simian virus 40 large tumor antigen transgenic mice. *Proc. Natl. Acad. Sci. U. S. A.* **90**:11029–11033.

51. Mason, R.J., Nellenbogen, J., and Clements, J.A. 1976. Isolation of disaturated phosphatidylcholine with osmium tetroxide. *J. Lipid Res.* **17**:281–284.

52. Bartlett, G.R. 1959. Phosphorus assay in column chromatography. *J. Biol. Chem.* **234**:466–468.

53. Stahlman, M.T., Gray, M.E., Hull, W.M., and Whitsett, J.A. 2002. Immunolocalization of surfactant protein-D (SP-D) in human fetal, newborn, and adult tissues. *J. Histochem. Cytochem.* **50**:651–660.

54. Dranoff, G., et al. 1994. Involvement of granulocyte-macrophage colony-stimulating factor in pulmonary homeostasis. *Science.* **264**:713–716.

55. Irizarry, R.A., et al. 2003. Exploration, normalization, and summaries of high density oligonucleotide array probe level data. *Biostatistics.* **4**:249–264.

56. Irizarry, R.A., et al. 2003. Summaries of Affymetrix GeneChip probe level data. *Nucleic Acids Res.* **31**:e15.

57. Benjamini, Y., and Hochberg, Y. 1995. Controlling the False Discovery Rate: a Practical and Powerful Approach to Multiple Testing. *Journal of the Royal Statistical Society. Series B.* **57**:289–300.

58. Dennis, G., Jr. et al., 2003. DAVID: Database for Annotation, Visualization, and Integrated Discovery. *Genome Biol.* **4**:P3.

59. Li, Z., et al. 2003. A global transcriptional regulatory role for c-Myc in Burkitt's lymphoma cells. *Proc. Natl. Acad. Sci. U. S. A.* **100**:8164–8169.

60. Hyatt, B.A., Shangguan, X., and Shannon, J.M. 2004. FGF-10 induces SP-C and Bmp4 and regulates proximal-distal patterning in embryonic tracheal epithelium. *Am. J. Physiol. Lung Cell. Mol. Physiol.* **287**:L1116–L1126.

61. Oka, T., Dai, Y.S., and Molkentin, J.D. 2005. Regulation of calcineurin through transcriptional induction of the calcineurin A beta promoter in vitro and in vivo. *Mol. Cell. Biol.* **25**:6649–6659.